International Journal of Power Electronics and Drive System (IJPEDS)
Vol. 9, No. 3, September 2018, pp. 1432~1444
ISSN: 2088-8694, DOI: 10.11591/ijpeds.v9.i3.pp1432-1444

Input Current Ripple Analysis of Multiphase PWM Inverters

Anwar Muqorobin, Pekik Argo Dahono
School of Electrical Engineering and Informatics, Institute of Technology Bandung, Indonesia

Article Info

Article history:

Received Mar 16, 2018
Revised Jul 5, 2018
Accepted Aug 6, 2018

Keyword:

Current ripple
Multiphase
PWM inverters

ABSTRACT

This paper investigates the relationship between inverter phase number and inverter input current ripple. Analysis results show that increasing the phase number more than nine cannot provide significant input current ripple reduction. The input current ripple is not affected by the switching frequency. Simulation and experimental results are included in this paper to show the validity of the proposed analysis method.

Corresponding Author:

Anwar Muqorobin,
School of Electrical Engineering and Informatics,
Institute of Technology Bandung,
Jl. Ganesha no. 10, Bandung, Indonesia.
Email: anwa006@students.itb.ac.id

1. INTRODUCTION

An electric motor with phase number more than three is called a multiphase motor. According to the phase number, multiphase motor can be divided into two types, i.e. prime phase motor and multiple three-phase motor [1]-[3]. Multiphase motor was firstly attempted to reduce torque pulsation that is inherent in squarewave inverter-fed three-phase motor. The first multiphase motor has shown that five-phase motor could reduce torque pulsation compared to three-phase motor [4]. It was also shown that asymmetrical stator winding configuration is useful to reduce torque pulsation in multiple three-phase motors [3]-[5]. Though torque pulsation is reduced by increasing the phase number, it was shown that the stator current ripple is increased. The stator current ripple can be reduced by using appropriate pulsewidth modulation (PWM) techniques. However, this reduction is not significant when the phase number is more than fifteen [6]-[7]. Another advantages of multiphase motor is torque enhancement when harmonic current injection is used. Compared to three-phase motor with equal size, the torque density of five-phase motor becomes 7.3% higher, for six-phase motor is 7%, seven-phase motor is 1.2% and eleven-phase motor is only 0.2% [8]-[9].

Different to three-phase inverter, just a few works on the input current ripple of multiphase PWM inverters have been published. Predetermination of input current ripple is important in selecting input DC filter capacitor. At present, DC filter capacitor is considered as the most unreliable component in power electronic systems. Although various modulation has been proposed to reduce the inverter output current ripple, it has no benefit on the input current ripple [10]-[11]. Further efforts show that the symmetrical configuration gives minimum input current ripple in multiple three phase PWM inverters [12]-[14]. Previous works also have shown that the input current ripple cannot be reduced by increasing the switching frequency but can be reduced by increasing the phase number [10]-[15]. Until now, however, no works have shown a general relationship between the input current ripple and phase number.

This paper presents a general relationship between the PWM inverter input current ripple and the phase number. A general expression of input current ripple as a function of inverter phase number is derived. It is found that nine phase is the maximum phase number that provides significant reduction on the inverter input current ripple. Simulated and experimental results are included to verify the proposed analysis method.

2. INPUT CURRENT RIPPLE ANALYSIS

In this section, input current ripple analysis of inverter-fed multiphase motor is detailed. The scheme of inverter-fed multiphase motor is shown in Figure 1. Two level voltage source inverter is used to drive the motor. A carrier based sinusoidal PWM is used to control the inverter. Sinusoidal reference signals are compared to a high frequency triangular carrier signal to produce ON-OFF signals for the inverter switching devices. If a reference signal is higher than the carrier signal, the associated upper (lower) switching device receives an ON (OFF) signal. The sinusoidal reference signals for multiphase inverter can be represented as:

$$v_m^r = k \sin(\theta + (m-1)\frac{2\pi}{n}) \quad (1)$$

In (1), v_m^r is the reference signal for phase m with m=1,2,3, ... n, n is the phase number, k is the modulation index, $\theta = 2\pi ft$, f is the inverter fundamental frequency, and t is time in second. The reference signals are plotted in Figure 2. From the figure it can be seen that generally the pattern is repeated every $2\pi/n$. This can be divided into two different patterns i.e. for odd and even phase number. In Figures 3 and 4, five-phase is used as representation of odd phase number and six-phase for even phase number.

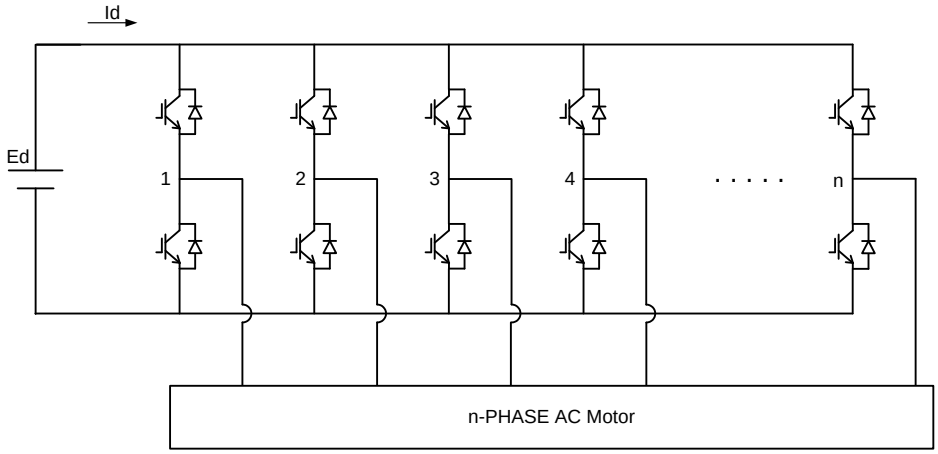

Figure 1. Inverter-fed multiphase motor

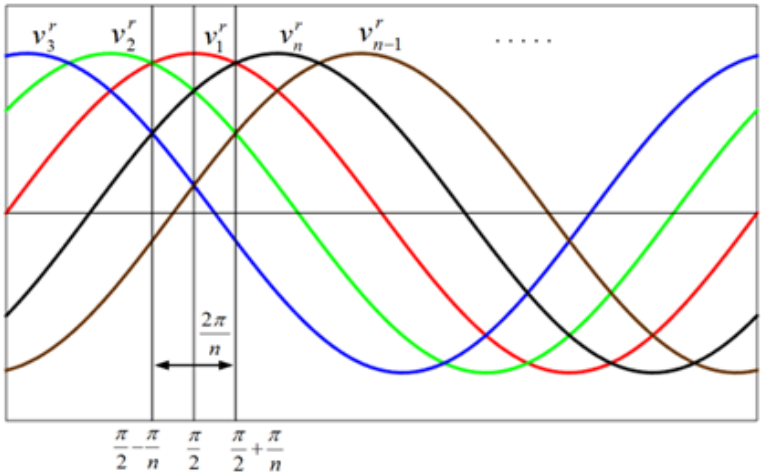

Figure 2. Reference signals of multiphase inverter

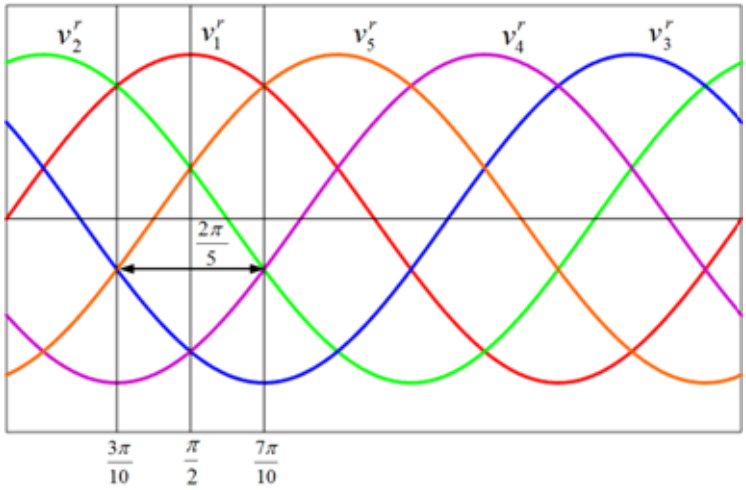

Figure 3. Reference signals of five-phase inverter

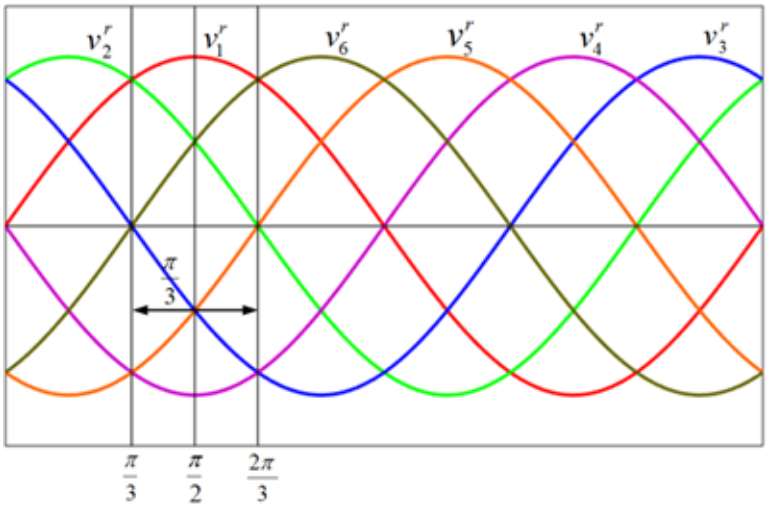

Figure 4. Reference signals of six-phase inverter

If the carrier signal frequency is much higher than the fundamental output frequency, the reference signals over one carrier period can be assumed as constants. The waveforms over one carrier period in the interval of $\pi/2 - \pi/n$ to $\pi/2$ for odd phase inverters are shown in Figure 5. Based on Figure 5, the time periods of T_0 to T_4 can be obtained as in (2)-(6).

$$\frac{T_0}{T_s} = \frac{1-v_1^r}{4} \quad (2)$$

$$\frac{T_1}{T_s} = \frac{v_1^r-v_2^r}{4} \quad (3)$$

$$\frac{T_2}{T_s} = \frac{v_2^r-v_n^r}{4} \quad (4)$$

$$\frac{T_3}{T_s} = \frac{v_n^r-v_3^r}{4} \quad (5)$$

$$\frac{T_4}{T_s} = \frac{v_3^r-v_{n-1}^r}{4} \quad (6)$$

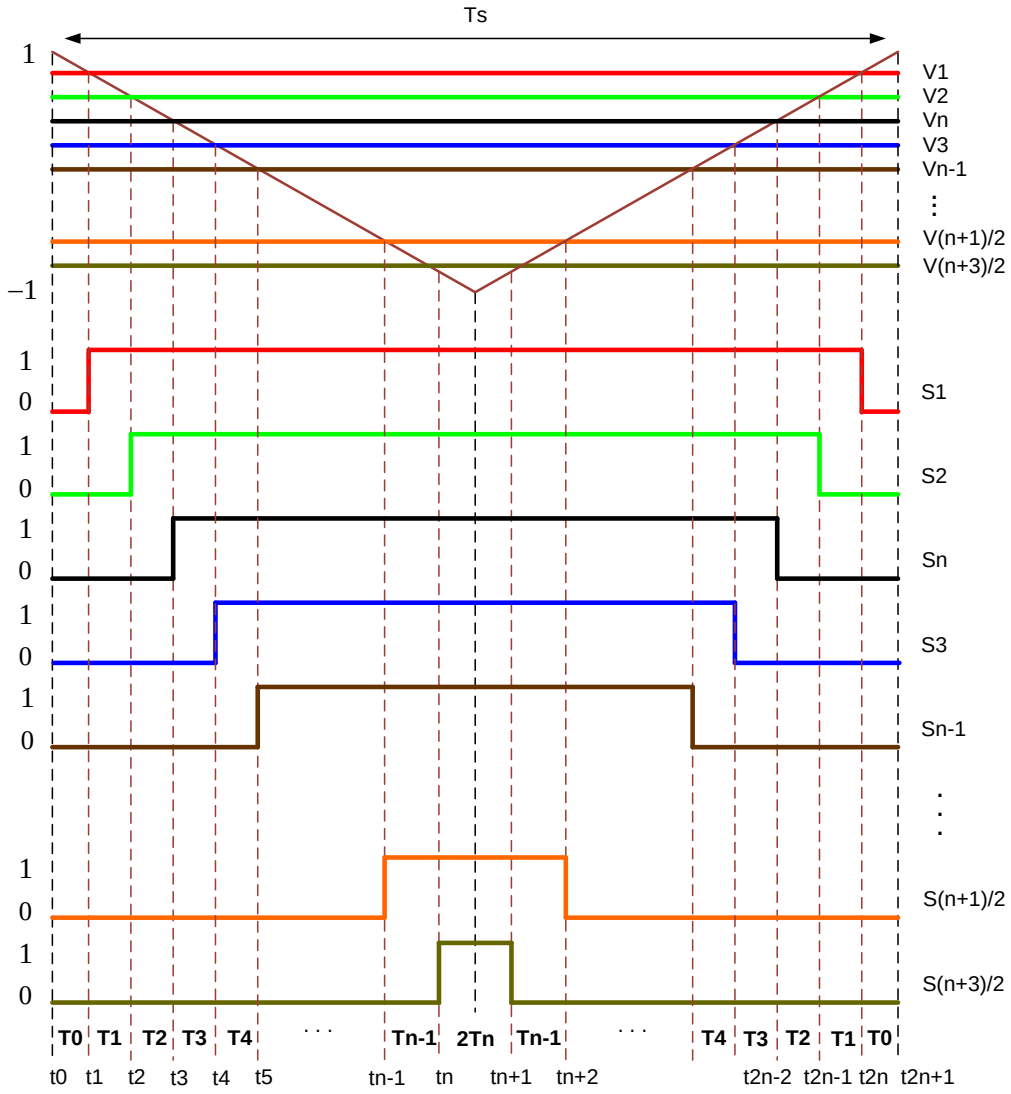

Figure 5. Detailed waveform during switching period

The time periods in (2) to (6) are continued until T_n. The periods of T_{n-1} and T_n can be represented as in (7) and (8).

$$\frac{T_{n-1}}{T_s} = \frac{v^r_{(n+1)/2} - v^r_{(n+3)/2}}{4} \quad (7)$$

$$\frac{T_n}{T_s} = \frac{1 + v^r_{(n+3)/2}}{4} \quad (8)$$

For inverter input current ripple analysis, it is assumed that the inverter input voltage is a constant DC voltage with no ripple and the inverter switching devices are ideal switches. Moreover, it is also assumed that the motor is a balanced multiphase motor. When the switching frequency is very high, the output currents can be assumed sinusoidal and can be written as:

$$i_m = \sqrt{2} I_l \sin(\theta + (m-1)\frac{2\pi}{n} - \phi) \quad (9)$$

In the above equations, I_l is the rms of output current, ϕ is the power factor angle, and i_m are the output current for phase m.

To calculate the input current ripple, firstly the input current is represented as a function of the output currents and the switching function of the inverter as follows.

$$i_d = S_1 i_1 + S_2 i_2 + S_3 i_3 + \cdots + S_{n-1} i_{n-1} + S_n i_n \tag{10}$$

Where S_m equal to one (zero) when the corresponding upper switching device receives an ON (OFF) signal. The input current during one switching period in Figure 5 can be written as shown by (11).

$$i_d = \begin{cases} 0 & , \quad t_0 \le t \le t_1 \\ i_1 & , \quad t_1 \le t \le t_2 \\ i_1 + i_2 & , \quad t_2 \le t \le t_3 \\ i_1 + i_2 + i_n & , \quad t_3 \le t \le t_4 \\ i_1 + i_2 + i_n + i_3 & , \quad t_4 \le t \le t_5 \\ \cdots & , \quad \cdots \\ \cdots & , \quad \cdots \\ i_1 + i_2 + i_n + i_3 + i_{n-1} + \ldots + i_{(n+1)/2} & , \quad t_{n-1} \le t \le t_n \\ 0 & , \quad t_n \le t \le t_{n+1} \\ i_1 + i_2 + i_n + i_3 + i_{n-1} + \ldots + i_{(n+1)/2} & , \quad t_{n+1} \le t \le t_{n+2} \\ \cdots & , \quad \cdots \\ \cdots & , \quad \cdots \\ i_1 + i_2 + i_n + i_3 & , \quad t_{2n-4} \le t \le t_{2n-3} \\ i_1 + i_2 + i_n & , \quad t_{2n-3} \le t \le t_{2n-2} \\ i_1 + i_2 & , \quad t_{2n-2} \le t \le t_{2n-1} \\ i_1 & , \quad t_{2n-1} \le t \le t_{2n} \\ 0 & , \quad t_{2n} \le t \le t_{2n+1} \end{cases} \tag{11}$$

The mean square value of the input current in one switching period can be obtained as:

$$I_d^2 = \frac{1}{T_s} \int_{t_0}^{T_s + t_0} i_d^2 dt \tag{12}$$

$$I_d^2 = \frac{2}{T_s} \begin{bmatrix} (i_1)^2 T_1 + (i_1 + i_2)^2 T_2 + (i_1 + i_2 + i_n)^2 T_3 \\ + (i_1 + i_2 + i_n + i_3)^2 T_4 + \ \ldots + \\ \left(i_1 + i_2 + i_n + i_3 + i_{n-1} + \ldots + i_{(n+1)/2}\right)^2 T_{n-1} \end{bmatrix} \tag{13}$$

and its average value over one fundamental period is obtained as:

$$I_{d,av}^2 = \frac{n}{\pi} \int_{\frac{\pi}{2} - \frac{\pi}{n}}^{\frac{\pi}{2}} I_d^2 d\theta \tag{14}$$

Finally the mean square value of the input current ripple can be obtained as:

$$\tilde{I}_d^2 = I_{d,av}^2 - \bar{I}_d^2 \tag{15}$$

Where

$$\bar{I}_d = n \frac{k}{2\sqrt{2}} I_l \cos \phi \tag{16}$$

is the DC component of the input current.

The resulted input current ripple of odd phase number inverter is

$$\tilde{I}_d^2 = \frac{k I_l^2}{\pi} \left[\frac{4n}{3} \left(\sum_{p=1}^{\frac{n-1}{2}} \sin\left(\frac{p\pi}{n}\right) \right) \cos^2 \phi + \frac{2n}{3} \left(\sum_{p=1}^{\frac{n-1}{2}} q \sin\left(\frac{p\pi}{n}\right) \right) \right] - \frac{n^2}{8} k^2 I_l^2 \cos^2 \phi \tag{17}$$

With the values of q are shown in Table 1.

Table 1. The Values of q

p	$\frac{n-1}{2}$	$\frac{n-3}{2}$	$\frac{n-5}{2}$	$\frac{n-7}{2}$	$\frac{n-9}{2}$	$\frac{n-11}{2}$	...	2	1
q	-1	2	-1	-1	2	-1	...	...	...

The input current ripple of odd multiple three phase inverter can be obtained by following the similar procedure of odd phase number inverter. The resulted input current ripple is in (18).

$$\tilde{I}_d^2 = \frac{kI_l^2}{\pi}\left[\frac{4n}{3}\left(\sum_{p=1}^{\frac{n-1}{2}} \sin\left(\frac{p\pi}{n}\right)\right)\cos^2\phi - \frac{n}{3}\left(\sum_{p=1}^{\frac{n-1}{2}} q\sin\left(\frac{p\pi}{n}\right)\right)\right] - \frac{n^2}{8}k^2I_l^2\cos^2\phi \quad (18)$$

For even phase number e.g. 6, 12, 18 and 24 phase inverters, the reference pattern can be seen in Figure 4. The time intervals are equal to (2) to (6) and (7) and (8) are replaced with (19) and (20).

$$\frac{T_{n-1}}{T_s} = \frac{v^r_{(n+2)/2} - v^r_{(n+4)/2}}{4} \quad (19)$$

$$\frac{T_n}{T_s} = \frac{1 + v^r_{(n+4)/2}}{4} \quad (20)$$

Different to odd phase inverter, the average value should be evaluated over $2\pi/n$. The resulted input current ripple is a combination of the input current ripple of $(n+1)$ phase inverter and $(n-1)$ phase inverter, i.e.

$$\tilde{I}_d^2 = \frac{kI_l^2}{\pi}\left[\frac{2n}{3}\left(\sum_{p=1}^{\frac{n}{2}} \sin\left(\frac{p\pi}{n}\right) + \sum_{p=1}^{\frac{n}{2}-1} \sin\left(\frac{p\pi}{n}\right)\right)\cos^2\phi + \frac{n}{3}\left(\sum_{p=1}^{\frac{n}{2}} r_1\sin\left(\frac{p\pi}{n}\right) + \sum_{p=1}^{\frac{n}{2}-1} r_2\sin\left(\frac{p\pi}{n}\right)\right)\right] - \frac{n^2}{8}k^2I_l^2\cos^2\phi \quad (21)$$

This can be simplified to be (22).

$$\tilde{I}_d^2 = \frac{kI_l^2}{\pi}\left[\frac{2n}{3}\left(1 + 2\sum_{p=1}^{\frac{n}{2}-1} \sin\left(\frac{p\pi}{n}\right)\right)\cos^2\phi + \frac{n}{3}\left(\sum_{p=1}^{\frac{n}{2}} r\sin\left(\frac{p\pi}{n}\right)\right)\right] - \frac{n^2}{8}k^2I_l^2\cos^2\phi \quad (22)$$

with the values of r_1, r_2, and r are shown in Table 2.

Table 2. The Values of r_1, r_2, and r

p	$\frac{n}{2}$	$\frac{n}{2}-1$	$\frac{n}{2}-2$	$\frac{n}{2}-3$	$\frac{n}{2}-4$	$\frac{n}{2}-5$	...	2	1
r_1	-1	2	-1	-1	2	-1	...	...	...
r_2		-1	2	-1	-1	2	...	...	...
r	-1	1	1	-2	1	1	...	...	...

It can be seen from (17), (18), and (22) that the input current ripple is not affected by the switching frequency. Thus, the input current ripple cannot be reduced by increasing the switching frequency. By using (17), (18), and (22), the resulted input current ripple for multiphase inverter with phase numbers of 3 to 17 are shown in Table 3.

Table 3. Input Current Ripple of Multiphase PWM Inverters

Phase number	Input current ripple $\tilde{I}_d^2$
3	$\frac{kI_l^2}{\pi}\left[2\sqrt{3}\cos^2\phi+\frac{\sqrt{3}}{2}\right]-\frac{9}{8}k^2I_l^2\cos^2\phi$
5	$\frac{kI_l^2}{\pi}\left[\begin{matrix}\frac{20}{3}\left(\sin\left(\frac{2\pi}{5}\right)+\sin\left(\frac{\pi}{5}\right)\right)\cos^2\phi\\+\frac{10}{3}\left(-\sin\left(\frac{2\pi}{5}\right)+2\sin\left(\frac{\pi}{5}\right)\right)\end{matrix}\right]-\frac{25}{8}k^2I_l^2\cos^2\phi$
6	$\frac{kI_l^2}{\pi}\left[\begin{matrix}\frac{12}{3}\left(1+2\sin\left(\frac{2\pi}{6}\right)+2\sin\left(\frac{\pi}{6}\right)\right)\cos^2\phi\\+\frac{6}{3}\left(-\sin\left(\frac{3\pi}{6}\right)+\sin\left(\frac{2\pi}{6}\right)+\sin\left(\frac{\pi}{6}\right)\right)\end{matrix}\right]-\frac{36}{8}k^2I_l^2\cos^2\phi$
7	$\frac{kI_l^2}{\pi}\left[\begin{matrix}\frac{28}{3}\left(\sin\left(\frac{3\pi}{7}\right)+\sin\left(\frac{2\pi}{7}\right)+\sin\left(\frac{\pi}{7}\right)\right)\cos^2\phi\\+\frac{14}{3}\left(-\sin\left(\frac{3\pi}{7}\right)+2\sin\left(\frac{2\pi}{7}\right)-\sin\left(\frac{\pi}{7}\right)\right)\end{matrix}\right]-\frac{49}{8}k^2I_l^2\cos^2\phi$
9	$\frac{kI_l^2}{\pi}\left[\begin{matrix}\frac{36}{3}\left(\sin\left(\frac{4\pi}{9}\right)+\sin\left(\frac{3\pi}{9}\right)+\sin\left(\frac{2\pi}{9}\right)+\sin\left(\frac{\pi}{9}\right)\right)\cos^2\phi\\-\frac{9}{3}\left(-\sin\left(\frac{4\pi}{9}\right)+2\sin\left(\frac{3\pi}{9}\right)-\sin\left(\frac{2\pi}{9}\right)-\sin\left(\frac{\pi}{9}\right)\right)\end{matrix}\right]-\frac{81}{8}k^2I_l^2\cos^2\phi$
11	$\frac{kI_l^2}{\pi}\left[\begin{matrix}\frac{44}{3}\left(\sin\left(\frac{5\pi}{11}\right)+\sin\left(\frac{4\pi}{11}\right)+\sin\left(\frac{3\pi}{11}\right)+\sin\left(\frac{2\pi}{11}\right)+\sin\left(\frac{\pi}{11}\right)\right)\cos^2\phi\\+\frac{22}{3}\left(-\sin\left(\frac{5\pi}{11}\right)+2\sin\left(\frac{4\pi}{11}\right)-\sin\left(\frac{3\pi}{11}\right)-\sin\left(\frac{2\pi}{11}\right)+2\sin\left(\frac{\pi}{11}\right)\right)\end{matrix}\right]-\frac{121}{8}k^2I_l^2\cos^2\phi$
12	$\frac{kI_l^2}{\pi}\left[\begin{matrix}\frac{24}{3}\left(1+2\sin\left(\frac{5\pi}{12}\right)+2\sin\left(\frac{4\pi}{12}\right)+2\sin\left(\frac{3\pi}{12}\right)+2\sin\left(\frac{2\pi}{12}\right)+2\sin\left(\frac{\pi}{12}\right)\right)\cos^2\phi\\\frac{12}{3}\left(-\sin\left(\frac{6\pi}{12}\right)+\sin\left(\frac{5\pi}{12}\right)+\sin\left(\frac{4\pi}{12}\right)-2\sin\left(\frac{3\pi}{12}\right)+\sin\left(\frac{2\pi}{12}\right)+\sin\left(\frac{\pi}{12}\right)\right)\end{matrix}\right]-\frac{144}{8}k^2I_l^2\cos^2\phi$
13	$\frac{kI_l^2}{\pi}\left[\begin{matrix}\frac{52}{3}\left(\sin\left(\frac{6\pi}{13}\right)+\sin\left(\frac{5\pi}{13}\right)+\sin\left(\frac{4\pi}{13}\right)+\sin\left(\frac{3\pi}{13}\right)+\sin\left(\frac{2\pi}{13}\right)+\sin\left(\frac{\pi}{13}\right)\right)\cos^2\phi\\+\frac{26}{3}\left(-\sin\left(\frac{6\pi}{13}\right)+2\sin\left(\frac{5\pi}{13}\right)-\sin\left(\frac{4\pi}{13}\right)-\sin\left(\frac{3\pi}{13}\right)+2\sin\left(\frac{2\pi}{13}\right)-\sin\left(\frac{\pi}{13}\right)\right)\end{matrix}\right]-\frac{169}{8}k^2I_l^2\cos^2\phi$
15	$\frac{kI_l^2}{\pi}\left[\begin{matrix}\frac{60}{3}\left(\sin\left(\frac{7\pi}{15}\right)+\sin\left(\frac{6\pi}{15}\right)+\sin\left(\frac{5\pi}{15}\right)+\sin\left(\frac{4\pi}{15}\right)+\sin\left(\frac{3\pi}{15}\right)+\sin\left(\frac{2\pi}{15}\right)+\sin\left(\frac{\pi}{15}\right)\right)\cos^2\phi\\-\frac{15}{3}\left(-\sin\left(\frac{7\pi}{15}\right)+2\sin\left(\frac{6\pi}{15}\right)-\sin\left(\frac{5\pi}{15}\right)-\sin\left(\frac{4\pi}{15}\right)+2\sin\left(\frac{3\pi}{15}\right)-\sin\left(\frac{2\pi}{15}\right)-\sin\left(\frac{\pi}{15}\right)\right)\end{matrix}\right]-\frac{225}{8}k^2I_l^2\cos^2\phi$
17	$\frac{kI_l^2}{\pi}\left[\begin{matrix}\frac{68}{3}\left(\sin\left(\frac{8\pi}{17}\right)+\sin\left(\frac{7\pi}{17}\right)+\sin\left(\frac{6\pi}{17}\right)+\sin\left(\frac{5\pi}{17}\right)+\sin\left(\frac{4\pi}{17}\right)+\sin\left(\frac{3\pi}{17}\right)+\sin\left(\frac{2\pi}{17}\right)+\sin\left(\frac{\pi}{17}\right)\right)\cos^2\phi\\+\frac{34}{3}\left(-\sin\left(\frac{8\pi}{17}\right)+2\sin\left(\frac{7\pi}{17}\right)-\sin\left(\frac{6\pi}{17}\right)-\sin\left(\frac{5\pi}{17}\right)+2\sin\left(\frac{4\pi}{17}\right)-\sin\left(\frac{3\pi}{17}\right)-\sin\left(\frac{2\pi}{17}\right)+2\sin\left(\frac{\pi}{17}\right)\right)\end{matrix}\right]-\frac{289}{8}k^2I_l^2\cos^2\phi$

3. COMPARISON

Figures 6 and 7 show the inverter input current ripple as a function of modulation index for power factors of 0.8 and 1.0, respectively. In these figures, the input current ripples of multiphase inverters are normalized with respect to three-phase inverters, with equal total output power. These figures show that under the same total output power, the input current ripple of the inverter is reduced with the increase of phase number. However, this reduction is not proportional to the phase number. A significant reduction is obtained when the phase number is increased from three to five. The reduction is higher when the modulation index is closed to one.

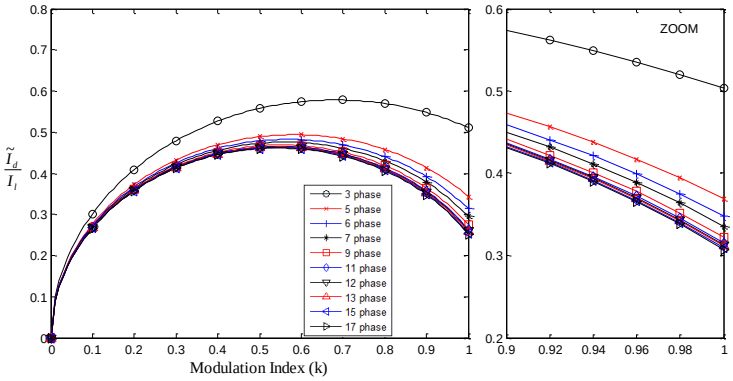

Figure 6. Input current ripple when PF=0.8

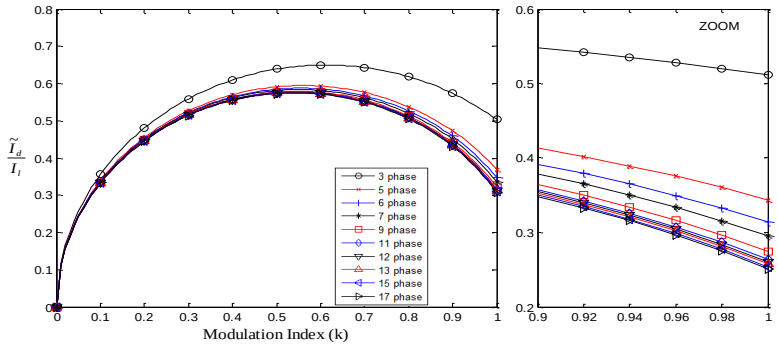

Figure 7. Input current ripple when PF=1.0

Figure 8 shows the normalized input current ripple value when the modulation index is one for both power factors. The figure shows that the input current ripple reduction is not significant when the phase number is more than nine. The phase number more than nine is suitable in application where another reasons e.g. reliability or power semiconductor rating are considered.

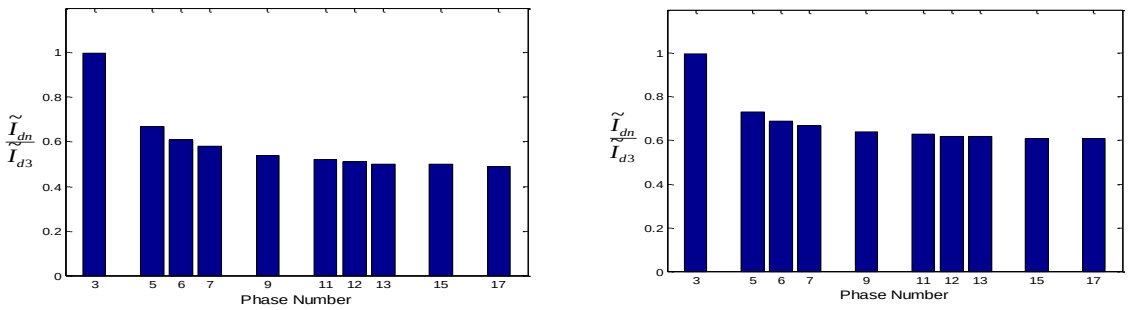

(a) (b)

Figure 8. Input current ripple when the modulation index is one (a) PF=0.8 and (b) PF=1.0

4. SIMULATION AND EXPERIMENTAL RESULTS

At first, simulation works are conducted to verify the proposed analysis method. For this purpose, a static RL load was assumed. A static RL load may represents an AC motor under locked rotor. The load for three phase inverter has resistance of 2 Ohm and inductance of 4.78 mH. Under 50 Hz of fundamental frequency, the load power factor is 0.8. The loads for other phase inverters are adjusted so that the same output powers are produced. The DC input for the inverters was set to 40 Vdc and the PWM uses a carrier frequency of 1 kHz. The simulation results when modulation index is 1.0 are presented in Figure 9. From the figure, it can be seen clearly that multiphasing could reduce the input current ripple and the reduction become insignificant when the phase number is more than nine.

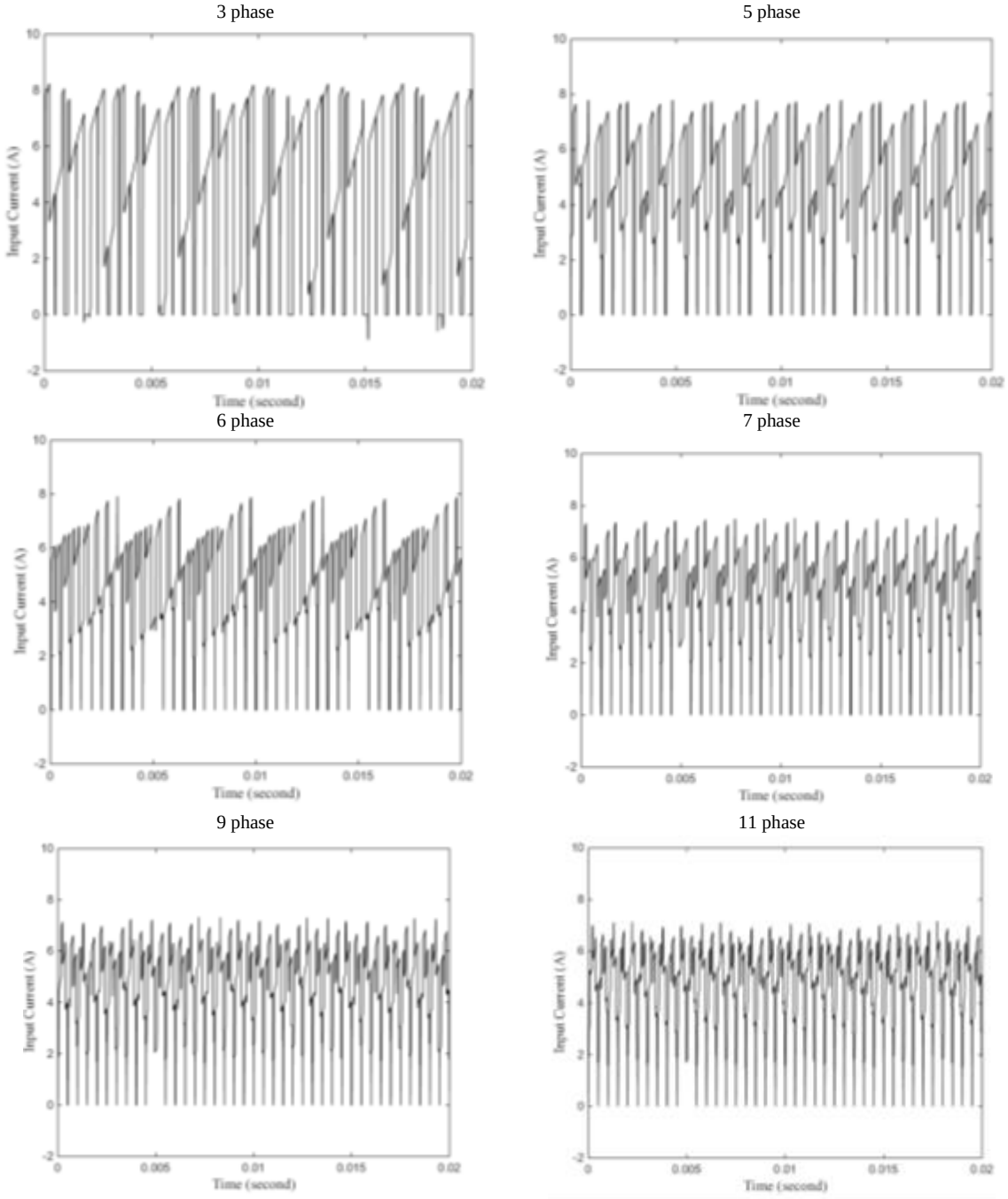

Figure 9. Simulation results of input current when the modulation index is one

The experimental set up is shown in Figure 10. The inverter switching devices use power mosfets. The PWM uses carrier frequency of 1 kHz and implemented by using FPGA ALTERA DE2-70. The experiments were carried out using six-phase and nine-phase motors. Both motors are locked during the experiments. Under locked rotor, the inductance of the six-phase motor is 12.52 mH and the resistance is 2.7 Ohm. For the nine-phase motor, the inductance is 10.04 mH and the resistance is 1.78 Ohm. The DC input for the inverters was set to 40 Vdc. The input current ripple is measured by using a digital oscilloscope then the results are processed by using a digital computer.

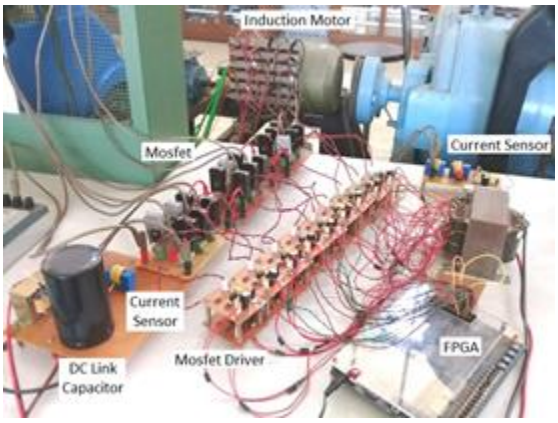

Figure 10. Experimental setup

The experimental results of six-phase and nine-phase inverters are shown in Figure 11. Modulation index of 1.0 is used for these waveforms. From the figures, it is known that the output current almost sinusoidal eventhough the switching frequency is not high. The waveforms of the input currents in Figure 11 that are plotted during fundamental period are shown in Figure 12. From this figure and Figure 9, good agreement between simulation and experimental waveforms can be observed easily. The calculated input current ripples for modulation index of 0.2 to 1.0 are shown in Figure 13 and 14, each for six and nine-phase inverters, respectively. From these figures, very good agreement between the calculated and experimental results can be appreciated.

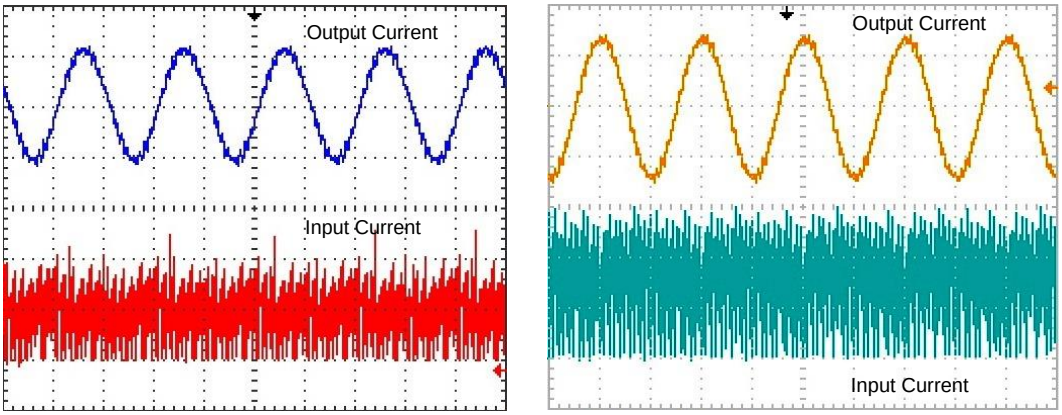

(a) (b)

amp/div=4 A time/div=10 ms

Figure 11. Output current and input current of (a) six-phase inverter and (b) nine-phase inverter

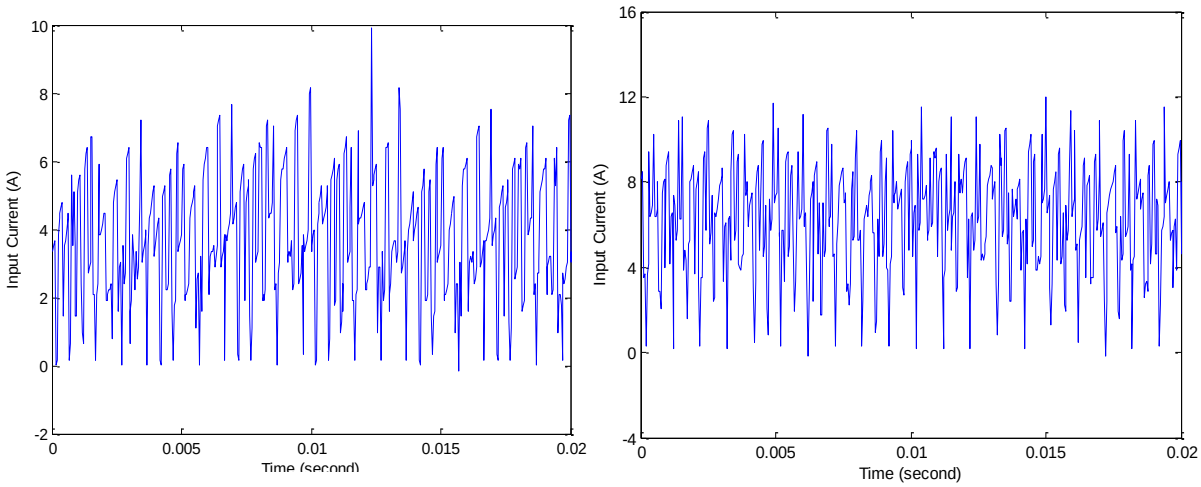

(a) (b)

Figure 12. Input current of (a) six-phase inverter and (b) nine-phase inverter

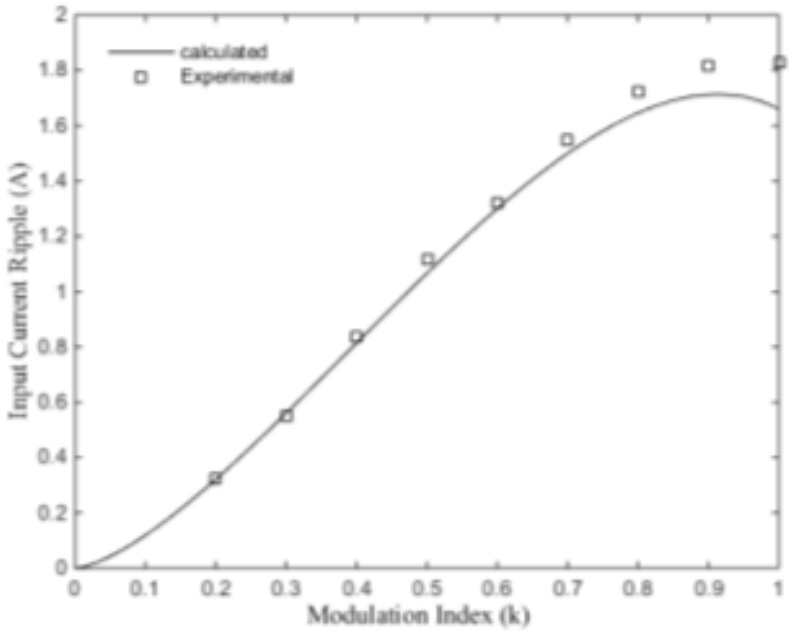

Figure 13. Input current ripple of six-phase inverter

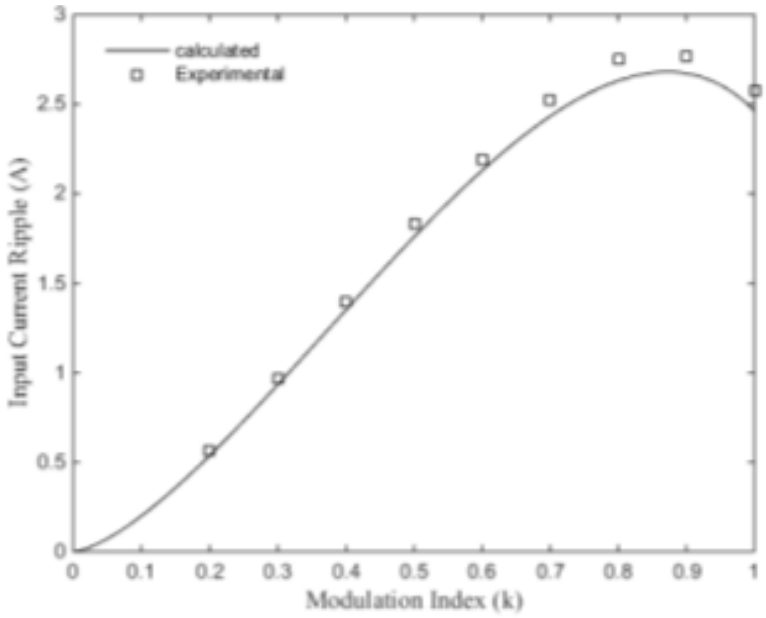

Figure 14. Input current ripple of nine-phase inverter

5. CONCLUSION

An input current ripple analysis method for multiphase PWM inverters has been proposed in this paper. It has been shown that the inverter input current ripple can be reduced by increasing the phase number. However, the reduction is not significant when the phase number is more than nine. Input current ripple cannot be reduced by increasing the switching frequency. Simulated and experimental results have been included in this paper to verify the proposed analysis method.

ACKNOWLEDGEMENTS

The first author thanks to Research Center for Electrical Power and Mechatronics, Indonesian Institute of Sciences (P2 Telimek-LIPI) and Kemenristekdikti Indonesia for doctoral scholarship.

REFERENCES

[1] H.A. Toliyat, T.A. Lipo, and J.C. White, "Analysis of a concentrated winding induction machine for adjustable speed drive applications part 2 (motor design and performance)," *IEEE Trans. Energy Convers.*, vol. 6, no. 4, pp. 684-692, Dec. 1991.
[2] E. Levi, R. Bojoi, F. Profumo, H.A. Toliyat, and S. Williamson, "Multi-phase induction motor drives-a technology status review," *IET Elect. Power Appl.*, vol. 1, no. 4, pp. 489-516, Jul. 2007.
[3] E.A. Klingshirn, "High phase order induction motors-part I-description and theoretical considerations," *IEEE Trans. Power App. Syst.*, vol. PAS-102, no. 1, pp. 47-53, Jan. 1983.
[4] E.E. Ward and H. Harer, "Preliminary investigation of an invertor-fed 5-phase induction motor," *PROC. IEE*, vol. 116, no. 6, pp. 980-984, Jun. 1969.
[5] R.H. Nelson and P.C. Krause, "Induction machine analysis for arbitrary displacement between multiple winding sets," *IEEE Trans. Power App. Syst.*, vol. PAS-93, no. 3, pp. 841-848, May 1974.
[6] J. Apsley, S. Williamson, A. Smith, and M. Barnes, "Induction motor performance as a function of phase number," *Electric Power Applications*, vol. 153, no. 6, pp. 898-904, Nov. 2006.
[7] S. Williamson and S. Smith, "Pulsating torque and losses in multiphase induction machines," *IEEE Trans. Ind. Appl.*, vol. 39, no. 4, pp. 986-993, Jul./Aug. 2003.
[8] A.S. Abdel-Khalik, M.I. Masoud, S. Ahmed, and A.M. Massoud, "Effect of current harmonic injection on constant rotor volume multiphase induction machine stators: a comparative study," *IEEE Trans. Ind. Appl.*, vol. 48, no. 6, pp. 2002-2013, Nov./Dec. 2012.
[9] R.O.C. Lyra and T.A. Lipo, "Torque density improvement in a six-phase induction motor with third harmonic current injection," *IEEE Trans. Ind. Appl.*, vol. 38, no. 5, pp 1351-1360, Sep./Oct. 2002.
[10] P.A. Dahono, Deni, C.P. Akbarifutra, and A. Rizqiawan, "Input ripple analysis of five-phase pulsewidth modulated inverters," *IET Power Electron.*, vol. 3, no. 5, pp. 716-723, 2010.

[11] R. Bojoi, M.C. Caponet, G. Grieco, M. Lazzari, A. Tenconi, and F. Profumo, "Computation and measurements of the DC link current in six-phase voltage source PWM inverters for AC motor drives," in *Proc. Power Conversion Conference*, Osaka, 2002, pp. 953-958.
[12] R.S. Parlindungan and P.A. Dahono, "Input current ripple analysis of double stator AC drive systems," in *International Conference on Information Technology and Electrical Engineeing (ICITEE)*, Yogyakarta, 2013, pp. 370-374.
[13] D. Nurafiat and P.A. Dahono, "Input current ripple analysis of nine-phase PWM inverters," in *37th Annual Conference on IEEE Industrial Electronics Society (IECON)*, Melbourne, 2011, pp. 1378-1383.
[14] A. Muqorobin and P.A. Dahono, "Optimal displacement for nine phase inverter," in *Proceedings of the Joint International Conference on Electric Vehicular Technology and Industrial, Mechanical, Electrical and Chemical Engineering (ICEVT & IMECE)*, Surakarta, 2015, pp. 258-262.
[15] M. Lazzari, F. Profumo, A. Tenconi, and G. Grieco, "Analytical and numerical computation of RMS current stress on the DC link capacitor in multiphase voltage source PWM inverters," in *EPE*, Graz, 2001, pp. 1-10.